ARTICLES

Variation of the Resonant Transfer Rate When Passing from Nonadiabatic to Adiabatic Electron Transfer

V. Gladkikh and A. I. Burshtein*

Chemical Physics Department, Weizmann Institute of Science, Rehovot 76100, Israel

I. Rips

Department of Sciences, Holon Academic Institute of Technology, Holon 58102, Israel

Received: December 14, 2004; In Final Form: April 11, 2005

Two competing theories are used for bridging the gap between the nonadiabatic and the deeply adiabatic electron transfer between symmetric parabolic wells. For the high friction limit, a simple analytic interpolation is proposed as a reasonable alternative to them, well-fitted to the results of numerical simulations. It provides a continuous description of the electron transfer rate in the whole range of variation of the nonadiabatic coupling between the diabatic states. For lower friction, the original theories are used for the same goal. With an increase in coupling, the cusped barrier transforms into the parabolic one. Correspondingly, the pre-exponent of the Arrhenius transfer rate first increases with coupling, then levels off approaching the "dynamic solvent effect" plateau but finally reduces reaching the limit of the adiabatic Kramers theory for the parabolic barrier. These changes proceeding with a reduction in the particle separation affect significantly the spatial dependence of the total transfer rate. When approaching the contact distance, the exact rate becomes smaller than in the theory of dynamical solvent effects and much smaller than predicted by perturbation theory (golden rule), conventionally used in photochemistry and electrochemistry.

I. Introduction

The electron transfer rate is a fundamental property used in the theories of intramolecular and intermolecular reactions in dense media.[1−4] At high temperatures, the system motion is adiabatic everywhere except at the crossing point of the intersecting energy levels where the electron tunneling occurs. For electron exchange reactions, the potential surface consists of the two symmetric diabatic energy levels, which are commonly assumed to be parabolic (Figure 1). The free energy gap for electron transfer in both directions is zero, and the transfer rate is given by the conventional Arrhenius equation:

$$W = k\, e^{-(U-V)/T},\ U = \lambda/4 \tag{1.1}$$

Here, U is the energetic height of the crossing point, $2V$ is the nonadiabatic splitting of the energy levels 1 and 2 at this point, λ is the reorganization energy of transfer, and $k_B = 1$.

The preexponential factor, k, depends on the nonadiabatic coupling and the dynamic of motion along the reaction coordinate. The evaluation of this factor constitutes a complex problem that cannot be solved universally within a single theory. A number of theories have to be used to cover the whole domain of $k(V,\gamma)$ where γ is a friction along the reaction coordinate. This two-dimensional domain was used in a few works[5−7] to indicate the results of different theories and their mutual borders as shown in Figure 2, taken from ref 7. This figure establishes all of the results and their regions of applicability but does not provide bridging between them. Particularly, the variation of the prefactor k with the nonadiabatic coupling V at a fixed dissipation strength γ (in the vertical cross-section of the domain from bottom to top) is due to the monotonic increase of the coupling,

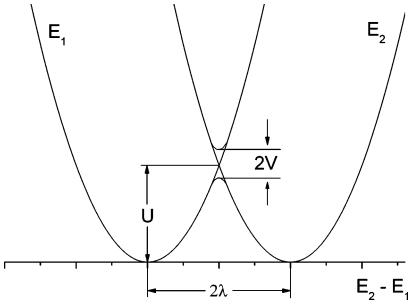

Figure 1. Energetic scheme of resonant electron transfer.

$$V(r) = V_0 e^{-(r-\sigma)/L} \tag{1.2}$$

with reduction of the inter-reactant separation (up to their closest approach at $r = \sigma$). Passing this way at high friction, one starts from the nonadiabatic perturbation theory subregion, where transfer is limited by tunneling, crosses the intermediate subregion of the dynamical solvent effect (DSE), but finishes in the adiabatic subregion where the reaction is controlled by

10.1021/jp044311y CCC: $30.25
Published on Web 05/18/2005

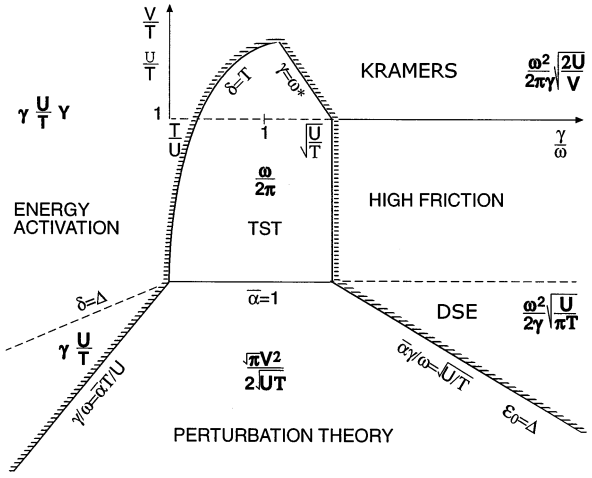

Figure 2. Entire domain of theoretical definitions of electron transfer pre-exponent $k(V,\gamma)$ given in ref 7. The vertical dashed line corresponds to the value $\lambda = 40T$ used further on.

diffusion to the crossing point. In each subregion, there are expressions for k, which differ from one another. The dependence of the preexponential factor $k[V(r)]$ is an essential part of the spatial dependence of $W(r)$ given in eq 1.1. As an input data used in the theories of intermolecular transfer,[3,4] it has to be continuous in r and not composed from a few pieces related to different theories valid at different distances. The main goal of the present work is to bridge these two pieces together to get a single continuous formula for the required $k(V)$ and $W(r)$ dependencies. It should be stressed that the urgent necessity to match the Fermi Golden Rule and Kramers high friction theory, including DSE, which separates them, was recognized long ago. At first, it was realized in the well-known Calef and Wolynes work[8] and then by means of the Pollak "variational transition state theory" (VTST).[9−12] In what follows, we will rely upon these two alternative approaches to the problem at hand.

Although the transfer is assisted by the system delivery to the crossing point, at sufficiently small V, it is limited everywhere not by this motion but by slow tunneling with the rate k_{PT}. The latter is given by the Fermi Golden Rule (second-order perturbation theory developed in ref 13; see also eqs 2.37 in ref 1 and 1.7 in ref 5):

$$k_{PT} = \frac{V^2}{\hbar}\sqrt{\frac{\pi}{\lambda T}} \tag{1.3}$$

However, at larger V, the tunneling ceases to control the reaction giving way to either energy activation at low friction ($\gamma \ll \omega$) or free vibrations at moderate friction (with the well frequency $\omega/2\pi$). At even larger values of the friction, the reaction is controlled by diffusion to the crossing point along the reaction coordinate. The last phenomenon was discovered independently in two simultaneously published papers, refs 14 and 15. The latter is addressed rather to the inner sphere low frequency vibrations such as in H-bonded complexes in water, studied later by pump−probe spectroscopy.[16−19] The former addressed more specifically the outer sphere electron transfer in Debye polar solvents where

$$\gamma = \omega^2 \tau_L \tag{1.4}$$

Here $\tau_L = \tau_D\, \epsilon_0/\epsilon$ is the longitudinal relaxation time of dielectric polarization related to the Debye relaxation time τ_D, through the ratio of the optical (ϵ_0) and static (ϵ) dielectric constants. Later on, the phenomenon of diffusional control in the reaction space, which became known as the dynamical solvent effect, was reproduced in a number of publications and observed experimentally.[20] However, with an increase in V, DSE gives way to the well-known Kramers result for the parabolic barrier. The latter is slightly different from DSE, which is actually its analogue for the cusped barrier:

$$k_{DSE} = 1/\tau_L\sqrt{\frac{\lambda}{16\pi T}} \text{ for the cusped barrier} \tag{1.5a}$$

$$k_{Kram} \simeq \frac{1}{\tau_L}\sqrt{\frac{\lambda}{8\pi^2 V}} \text{ for the parabolic one} \tag{1.5b}$$

In the present work, we focus mainly on the large friction (strong dissipation) region where the alternating formulas k_{PT}, k_{DSE}, and k_{Kram} follow one another with increasing V. There is also the more general expression derived by Zusman bridging between the first two:

$$k_{non} = \frac{k_{PT}\, k_{DSE}}{k_{PT} + k_{DSE}} = \begin{cases} k_{PT} & \text{weak nonadiabatic} \\ k_{DSE} & \text{strong nonadiabatic} \end{cases} \tag{1.6}$$

This is an exact solution of the sudden modulation equations used in refs 5, 14, and 15. There, the transfer was considered as nonadiabatic but weak where the perturbation theory holds and strong where it gives way to DSE. Later on, the two expressions (1.5) were also bridged by considering both of them as adiabatic transfer (along a quasi-ballistic mode) over either the cusped barrier or the parabolic one. The former transforms to the latter with an increase of the level splitting $2V$. This matching resulting in the general expression for the diffusion-assisted reaction k_{DAR} was first made by Calef and Wolynes[8] and later by Starobinets, Rips, and Pollak.[11] These approximations will be considered in the next section, and the simple interpolation formulas will be introduced for the large friction limit. In section III, these formulas will be bridged with that for perturbation theory for getting the final $k(V)$ and corresponding $W(r)$ dependencies. In section IV, we will do the same but will account for the spatial dependence of the reorganization energy peculiar for highly polar solvents. In the conclusions, we will summarize all of the results and outline the remaining problems.

It should be emphasized that in this paper we focus on high temperature, high barrier electron exchange reactions in Debye polar solvents. This implies that the reaction is thermally activated with electron tunneling proceeding in the vicinity of the crossing point of the diabatic potential surfaces. The solvent modes can be treated classically (nuclear tunneling is negligible). Furthermore, the effect of the high frequency quantum solvent modes is neglected.

II. Diffusion-Assisted Reaction

The matching alternative adiabatic results (1.5) allows covering the whole domain of diffusion-assisted transfer. An important generalization of this kind made by Calef and Wolynes[8] results in the following equation for the pre-exponent:

$$k_{CW} = \frac{\omega}{2\pi}\left\{\sqrt{1 + \frac{J^2}{2\pi\alpha}} - \frac{J}{\sqrt{2\pi\alpha}}\right\} \tag{2.1}$$

where

$$J(V,\lambda) = e^{V/T}\int_0^{\lambda/2T} dy\, \exp\left[\frac{y^2}{\lambda/T} - \sqrt{y^2 + (V/T)^2}\right] \tag{2.2}$$

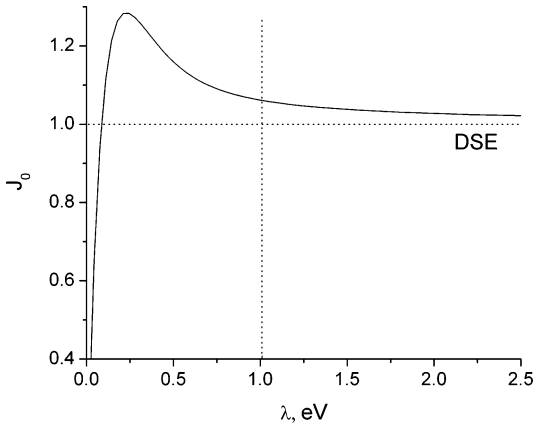

Figure 3. Correction factor for a cusped barrier rate, J_0, as a function of the reorganization energy.

and the dimensionless dissipative parameter

$$\alpha = \frac{\lambda}{2T}\left(\frac{\omega}{\gamma}\right)^2 \tag{2.3}$$

In general, the theory of Calef and Wolynes is valid from the intermediate (TST) to high friction (DSE) region (see Figure 2), so that

$$k_{\mathrm{CW}} = \begin{cases} \dfrac{\omega}{2\pi} = k_{\mathrm{TST}} & \gamma/\omega \ll \sqrt{\lambda/4T} \quad (\alpha \gg 2) \\ \dfrac{k_{\mathrm{DSE}}}{J(V,\lambda)} = k_\infty & \gamma \to \infty \qquad\qquad (\alpha \to 0) \end{cases} \tag{2.4}$$

but it is the best for the highest available friction (at $\alpha \to 0$). This is actually the case in which we are mainly interested.

In this particular case, the motion along the reaction coordinate to the crossing point is diffusional but it delivers the system to either a cusped or a quasi-parabolic barrier depending on whether the level splitting at the point is small or large, respectively. In the cusped barrier limit ($V \to 0$), the expression (2.2) reduces to the following one:

$$J(0, \lambda) = -\pi i \sqrt{\lambda/4T}\, e^{-\lambda/4T}\, \mathrm{erf}(i\sqrt{\lambda/4T}) = J_0(\lambda) \tag{2.5}$$

Although J_0 is real and positive, it is not equal to 1 at any finite barrier height $\lambda/4$, that is in general $k_\infty \neq k_{\mathrm{DSE}}$ even at $V \to 0$. As seen from Figure 3, J_0 approaches unity only as $\lambda \to \infty$. Otherwise

$$k_\infty = \begin{cases} k_{\mathrm{DSE}}/J_0(\lambda) = k_{\mathrm{CUSP}} & V \to 0 \\ \dfrac{1}{2\pi\tau L}\sqrt{\dfrac{\lambda}{2V} - 1} = k_{\mathrm{PAR}} & V \to \infty \end{cases} \tag{2.6}$$

The latter result is the more precise Kramers formula for a parabolic barrier. It differs slightly from its simplified version (1.5b) obtained for $2V \ll \lambda$. If V is not negligible (although smaller than $\lambda/2 = 2U$), then k_{PAR} should be used instead of eq 1.5b. Unlike the latter, it is nonlinear in the $\sqrt{T/V}$ coordinate of Figure 4.

It is easy to interpolate between the opposite limits represented in eq 2.6 to get a simple analytic alternative to the Calef and Wolynes k_∞ from eq 2.4:

$$k_{\mathrm{DAR}} = \frac{1}{\tau_{\mathrm{L}}}\sqrt{\frac{\lambda - 2V}{8\pi(2TJ_0^{\,2} + \pi V)}} = \begin{cases} k_{\mathrm{CUSP}} & \text{at } V \ll T \\ k_{\mathrm{PAR}} & \text{at } V \gg T \end{cases} \tag{2.7}$$

This is the pre-exponent of the diffusion-assisted rate of electron transfer over the barrier of arbitrary shape: from a cusped to a parabolic one. As can be seen in Figure 4, this interpolation not only approaches both these limits as expected but between goes through four points numerically calculated in ref 11.

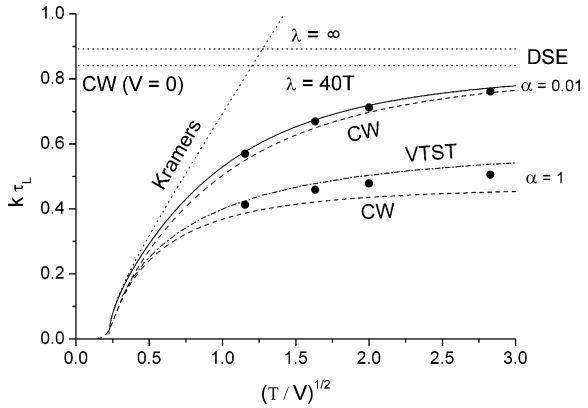

Figure 4. Pre-exponent k of diffusion-assisted electron transfer between the limits of cusped ($T/V \gg 1$) and parabolic ($T/V \ll 1$) barriers. The Kramers result for the latter is shown by the inclined dotted line while the horizontal dotted and dashed−dotted lines represent the DSE results for $\lambda = \infty$ and $\lambda = 40T$, respectively. All other curves are the following: our interpolation (solid line), Calef and Wolynes k_∞ for high and moderate friction (dashed lines), and VTST theory for the latter one (dash-dotted). The points represent the exact results obtained in ref 11 by numerical simulations for large ($\alpha = 0.01$) and moderate friction ($\alpha = 1.0$).

In the relatively low friction region, the better alternative to the Calef and Wolynes approximation is provided by VTST, which represents the pre-exponent in the following form:

$$k_{\mathrm{VTST}} = \frac{P}{2\pi\tau_{\mathrm{L}}}\sqrt{\frac{\lambda}{2\alpha T}} \tag{2.8}$$

and $P \equiv P(\alpha, V)$ has to be determined by solving the optimization problem as described in ref 11. Making this numerically, we found that the VTST curve $k(V)$ is very close to the four green points obtained for lower friction by numerical simulations made in ref 11. There, the reactive flux method[21] was employed for the integration of the Langevin equation of motion using the velocity Verlet algorithm.[22]

The black points in Figure 4 were calculated for $\alpha = 0.01$, that is for $\gamma/\omega \approx 45$ at $\lambda/T = 40$. This friction is large enough to be well-approximated by the Calef and Wolynes (CW) expression for k_∞. As for the green points, they were obtained in the same way and for the same λ/T but for $\alpha = 1$ when $\gamma/\omega \approx 4.5$. Here, we are very close to the boundary of the high friction region. As seen from Figure 2 in our case ($\lambda/T = 40$), this border is located at $\gamma/\omega = \sqrt{\lambda/4T} = \sqrt{10}$, that is far to the left from the cross-section $\gamma/\omega = 45$ to which we mainly address. The green points for the modest friction are somewhat better approximated by VTST than by the CW theory, while the black points for the higher friction are equally well-approximated by the original CW theory and our interpolation (2.7). However, the latter will be solely used further on just because of its relative simplicity.

III. General Interpolation

As a matter of fact, the cusp limit of either approximation (2.6) or interpolation (2.7) is never achieved in reality because at small V the limited stage of the transfer becomes not a

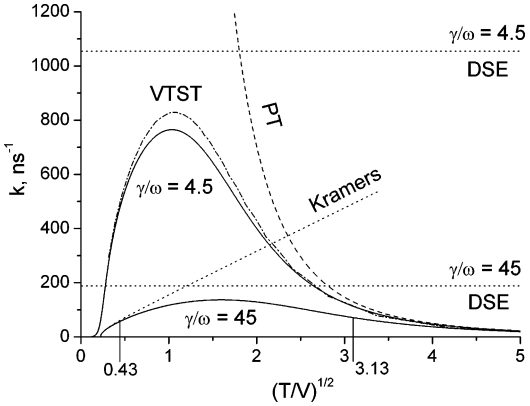

Figure 5. Solid curves are our interpolation (3.1) between the weak tunneling and the diffusion-assisted transfer. The former is given by the perturbation theory (PT, dashed line) while the latter is given by the Kramers and DSE approximation (dotted lines). The lowest solid line is our interpolation at high friction ($\alpha = 0.01$, $\gamma/\omega = 45$) while the upper dotted horizontal line over it represents the DSE approximation. Above them there are the similar lines for the lower friction ($\alpha = 1.0$, $\gamma/\omega = 4$, 5). The bottom vertical lines indicate the lower limits for the argument (3.13 and 0.43) accessible in two systems studied in refs 23 and 24, respectively.

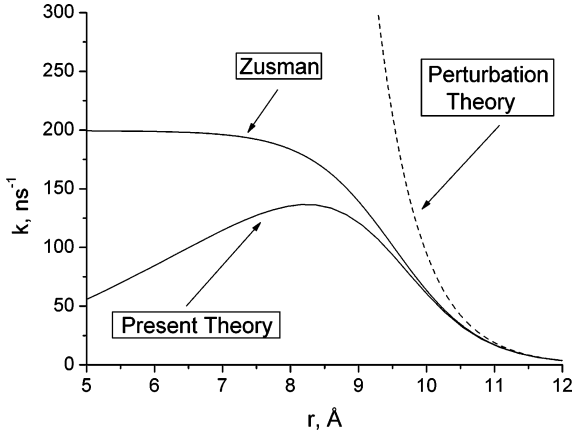

Figure 6. Pre-exponent k in different theories as a function of the interparticle distance at large friction ($\gamma/\omega = 45$) and $V_0 = 0.138$ eV, $L = 1.24$ Å.

diffusion to the crossing point but an electron tunneling. This means that the adiabatic theory should give way to the perturbation one as DSE does in the Zusman formula (1.6). Hence, to get the interpolation valid at any V, we just have to substitute k_{DSE} in this formula for k_{DAR} from eq 2.7:

$$k = \frac{k_{PT}\, k_{DAR}}{k_{PT} + k_{DAR}} \tag{3.1}$$

At small V, this constant is equal to k_{PT}, which is independent of friction unlike the longitudinal relaxation time τ_L, which increases with γ. At given $\omega = 10^{13}$, we obtain from the definition (1.4):

$$\frac{1}{\tau_L} = \omega\frac{\omega}{\gamma} = \begin{cases} 0.022\omega = 2.2 \times 10^{11}\ \mathrm{s}^{-1} & \text{at } \gamma/\omega = 45\ (\alpha = 0.01) \\ 0.22\omega = 2.2 \times 10^{12}\ \mathrm{s}^{-1} & \text{at } \gamma/\omega = 4.5\ (\alpha = 1) \end{cases} \tag{3.2}$$

Correspondingly, the height of the DSE plateau is higher the smaller is the friction (see Figure 5), but this plateau is never achieved by $k(V)$, which lowers with increasing V approaching the Kramers limit for the parabolic barrier. As a result, k is never as high as its DSE value but the very existence of this plateau as well as Kramers limit greatly reduces the actual k as compared with PT. However, the real deviation from the letter is not too large if $V \leq V_0 \ll T$, which is usually the case. For instance, T/V_0 calculated from the contact transfer rate obtained in ref 23 is equal to 3.13. As seen from Figure 5 at this point (in contact), k is only half of the perturbation theory value and this difference reduces quickly with increasing intermolecular distance. Only recently the system was encountered (perylene + TCNE) where the contact coupling is larger than T, namely, $T/V_0 = 0.43$.[24] There instead of the perturbation theory rate W_{PT} the Zusman formula (1.6) was used to account for DSE. However, at the highest $V = V_0$, even this correction is not enough. As seen from Figure 5 at this point, the Kramers high friction region is actually reached where the true k is twice smaller than its DSE alternative, not speaking about a much larger perturbation theory value.

To get an impression of what happens for lower friction, we used the same approach substituting k_{DSE} in the Zusman formula (1.6) by either k_{CW} from eq 2.4 or k_{VTST} from eq 2.8:

$$k = \frac{k_{PT}\, k_{CW}}{k_{PT} + k_{CW}} \text{ or } k = \frac{k_{PT}\, k_{VTST}}{k_{PT} + k_{VTST}} \tag{3.3}$$

Both of these results are also shown in Figure 5. The discrepancy between them is within the limits of accuracy of both approximations. The electron transfer rate increases with decreasing friction due to acceleration of the motion along the reaction coordinate. At a further decrease of friction, this motion becomes ballistic, and the transfer rate reaches its upper limit established by a plateau $k = k_{TST} = \omega/2\pi$. This plateau is not shown in Figure 5 because it is too high. Furthermore, we are interested in quite the opposite limit of the large friction available, where our interpolation (2.7) is the best.

In general, the importance of the diffusion control of the transfer increases with the increasing nonadiabatic coupling at contact. This effect is very impressive, especially if considered in real space. Using expression 1.2, we transformed into this space (Figure 6) the result obtained for the large friction $\gamma/\omega = 45$. It should be noted that in the vast majority of papers on intermolecular electron transfer, only the perturbation theory was so far used.[3,4] This is reasonable if either the electron coupling is much weaker than in the present example or the closest approach distance is much larger ($\omega > 10$ Å). In ref 24, for the first time, these conditions were shown to be broken in the system studied experimentally. There, only the use of the Zusman eq 1.6 instead of the perturbation theory allowed us to obtain a reasonable fit to the experimental data. However, Figure 6 shows that being better than perturbation theory, the Zusman approximation still overestimates the transfer rate at short distances where the barrier becomes parabolic. For attainment of the highest reliability of the fitting, the use of the present theory is essential. In the following section, we will see how it changes the real rate of transfer $W(r)$ given by eq 1.1.

IV. Transfer Rate in Polar Solvents

The reorganization energy employed in the foregoing analysis was considered as a distance-independent parameter. This is true only for in nonpolar solvents where the inner sphere contribution to the reorganization energy is the dominant one: $\lambda \equiv \lambda_{in} = \text{const}$. In highly polar solvents, the situation is the opposite: the inner sphere contribution can be neglected as

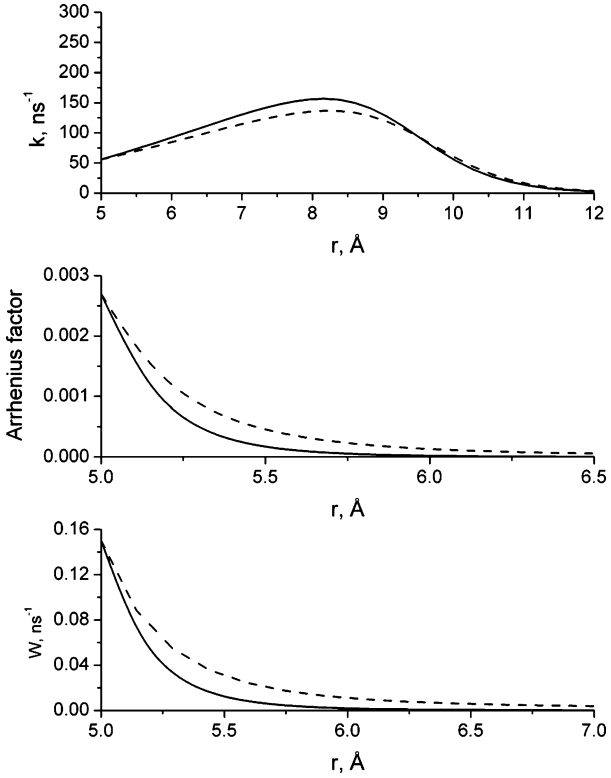

Figure 7. Pre-exponent, exponent, and their product W as functions of interparticle distance with (solid lines) and without (dashed lines) accounting for the space dependence of the reorganization energy.

compared with the outer sphere reorganization energy, which changes with distance between reactants according to the well-known law:[3,4]

$$\lambda(r) = \lambda_0(2 - \sigma/r) \tag{4.1}$$

In acetonitrile, the contact reorganization energy $\lambda_0 = 1.15$ eV and the average distance between contacting reactants is $\sigma = 5$ Å, if these are perylene and tetracyanoethylene (TCNE) as in ref 24.

Take into account that the $\lambda(r)$ dependence makes the pre-exponent k slightly larger in the adiabatic near contact region but smaller at larger separations, where the transfer is nonadiabatic (Figure 7). In parallel, $\lambda(r)$ dependence is responsible for the increase of $U(r) = \lambda(r)/4$ whose contact value is $U(\sigma) = \lambda_0/4$, while at infinite separation it is twice as large: $U(\infty) = \lambda_0/2$. As a result, the transfer rate

$$W(r) = k(r) \exp\left\{-\left[\frac{\lambda(r)}{4} - V(r)\right]/T\right\} \tag{4.2}$$

decreases with distance not only due to the pre-exponent but to increasing the activation energy as well.

Another important factor that affects the activation energy is the nonadiabatic coupling $V(r)$, which increases when approaching contact. As a result, the contact Arrhenius factor is significantly enhanced if $V_0 > T$, although it reduces sharply with increasing the inter-reactant distance. This effect is dominant at short distances where $V > T$, while at larger separation, the increase of $\lambda(r)$ contributes mainly to reduction of the Arrhenius factor.

The same tendency manifests itself in the reduction of $W(r)$, which is the product of $k(r)$ and the r-dependent Arrhenius factor (Figure 7). The spatial dependence of the transfer rate is

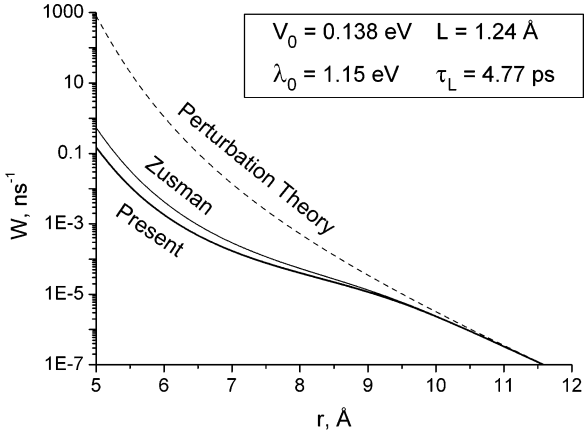

Figure 8. Space dependence of the transfer rates calculated with perturbation and Zusman theories and present interpolation.

significantly distorted, if the barrier reduction by $V(r)$ or $\lambda(r)$ dependence is ignored. In such a case, the kinetic rate constant

$$k_0 = \int W(r) d^3r$$

can be also overestimated as well as V_0 obtained by fitting the theory to the experimental data. Fortunately, the dispersion of reorganization energy is usually taken into account[3,4] and the lowering of the activation barrier was also accounted for when necessary.[25]

The diffusional control of the tunneling so far was considered only with the Zusman theory.[24,25] Now, we can estimate what is the difference between this and the present theory. In Figure 8, the present $W(r)$ is exhibited in the larger spatial interval than in Figure 7 and compared with the Zusman rate and that obtained using the Golden Rule (perturbation theory). Both our and the Zusman theories, which account for the diffusional control of the tunneling, and the rates of transfer at $r < 10$ Å are systematically lower than predicted by the perturbation theory. This difference ranges up to 3 orders of magnitude at the closest approach distance. The difference between the Zusman and our results is less pronounced but still runs as high as $3 \div 4$ times at $r < 6$ Å.

Special attention should be paid to the deviation of the true $W(r)$ dependence from its popular exponential approximation:

$$W(r) = W_0 e^{-(r-\sigma)/l} \tag{4.3}$$

In the limited range of distances, this simplification leads to a different and sometimes nonphysical value for W_0 and l. In particular, near the contact, l could be smaller than L, but in the medium larger than it and only as $r \rightarrow \infty$, the identity $l = L$ is reached. Too large values of l sometimes reported[26−29] are usually identified with L but associated with electron superexchange, which dominates the direct exchange of an electron.[30] However, it also may be an indication of too strong coupling, resulting in diffusional control of the transfer at short distances, making the dependence of the rate $W(r)$ on the distance less pronounced and leading to a natural excess of l over L. For instance, the "local" $l = -2\,(\mathrm{d}\ln W/\mathrm{d}r)^{-1}$ reaches in our case 1.67 Å (at $r = 8.4$ Å) as compared to the true tunneling distance $L = 1.24$ Å (at $r \rightarrow \infty$).

V. Conclusions

On a particular example of the resonant electron transfer, we have demonstrated that the Zusman account for the dynamical solvent effect is insufficient for determination of the transfer

rate if electron coupling at contact is too strong. Zusman's expression was generalized using the original interpolation between DSE and the adiabatic Kramers limit for high friction. The same was done for moderate values of the friction using two theories of diffusion-controlled electron transfer.[8,11] The present theory allows specifying the continuous distance dependence of the transfer rate from the infinite reactant separation and up to their closest approach where the maximal electron coupling is reached.

Although our analysis is quantitative only for the resonant transfer (with energy gap $\Delta G = 0$), it is qualitatively valid in the normal region ($-\Delta G < \lambda$) provided the transfer barrier

$$U = \frac{(\Delta G + \lambda)^2}{4\lambda} \tag{5.1}$$

does not differ significantly from $\lambda/4$. The situation changes qualitatively only in the inverted Marcus region ($-\Delta G > \lambda$). There, the dynamical solvent effect gives way to the sharp adiabatic cutoff of the transfer rate when electron coupling becomes too large. This situation was quantitatively described in ref 31 by eqs 53 and 28, which constitute an analogue of our eqs 3.1 or 3.3. A more complex situation arises at the boundary between the normal and the inverted region (at $-\Delta G = \lambda$), where the electron transfer is activationless ($U \approx 0$) and nonexponential.[32] The latter case deserves special consideration as well as the phonon-assisted electron transfer in the inverted region, which lowers the barriers, making one of the channels activationless.[3,4]

As already mentioned, our treatment of the nuclear motion of the solvent is classical, which is appropriate at high temperatures. At lower temperatures, nuclear tunneling has important physical effects on the electron transfer rate and should be taken into account.[33,34]

References and Notes

(1) Kuznetsov, A. M. *Charge Transfer in Physics, Chemistry and Biology*; Gordon & Breach: Amsterdam, 1995.
(2) May, V.; Kühn, O. *Charge and Energy Transfer Dynamics in Molecular Systems*; Wiley-VCH: Berlin, 2000.
(3) Burshtein, A. I. *Adv. Chem. Phys.* **2000**, *114*, 419.
(4) Burshtein, A. I. *Adv. Chem. Phys.* **2004**, *129*, 105.
(5) Burshtein, A. I.; Yakobson, B. I. *High Energy Chem.* **1981**, *14*, 211 (*Khim. Vysok. Energ.* **1980**, *14*, 291).
(6) Burshtein, A. I.; Zharikov, A. A. *Chem. Phys.* **1991**, *152*, 23.
(7) Burshtein, A. I.; Georgievskii, Yu. *J. Chem. Phys.* **1994**, *100*, 7319.
(8) Calef, D. F.; Wolynes, P. G. *J. Phys. Chem.* **1983**, *87*, 3387.
(9) Pollak, E. *J. Chem. Phys.* **1990**, *93*, 1116.
(10) Rips, I.; Pollak, E. *J. Chem. Phys.* **1995**, *103*, 7912.
(11) Starobinets, A.; Rips, I.; Pollak, E. *J. Chem. Phys.* **1996**, *104*, 6547.
(12) Pollak, E. In *Theoretical Methods in Condensed Phase Chemistry*; Schwartz, S. D., Ed.; Kluwer Academic Publishers: Dordrecht, 2000; pp 1−46.
(13) Levich, V. G. *Adv. Electrochem. Eng.* **1965**, *4*, 249.
(14) Zusman, L. D. *Chem. Phys.* **1980**, *49*, 295.
(15) Yakobson, B. I.; Burshtein, A. I. *Chem. Phys.* **1980**, *49*, 385.
(16) Burshtein, A. I.; Chernobrod, B. M.; Sivachenko, A. Yu. *J. Chem. Phys.* **1998**, *108*, 9796.
(17) Burshtein, A. I.; Chernobrod, B. M.; Sivachenko, A. Yu. *J. Chem. Phys.* **1999**, *110*, 1931.
(18) Burshtein, A. I.; Sivachenko, A. Yu. *J. Chem. Phys.* **2000**, *112*, 4699.
(19) Burshtein, A. I.; Sivachenko, A. Yu. *J. Phys.: Condens. Matter* **2000**, *12*, 173.
(20) Zusman, L. D. *Zeits. Phys. Chem.* **1994**, *186*, 1.
(21) Hänggi, P.; Talkner, P.; Borkovec, M. *Rev. Mod. Phys.* **1990**, *62*, 251.
(22) Allen, M. P.; Tildesley, D. J. *Computer Simulation of Liquids*; Oxford University Press: New York, 1987.
(23) Gladkikh, V. S.; Tavernier, H. L.; Fayer, M. D. *J. Phys. Chem. A* **2002**, *106*, 6982.
(24) Gladkikh, V. S.; Burshtein, A. I.; Angulo, G.; Pagès, S.; Lang, B.; Vauthey, E. *J. Phys. Chem. A* **2004**, *108*, 6667.
(25) Gladkikh, V. S.; Burshtein, A. I.; Feskov, S. V.; Ivanov, A. I.; Vauthey, E. In press.
(26) Killesreiter, H.; Baessler, H. *Chem. Phys. Lett.* **1971**, *11*, 411.
(27) Kuhn, H. *J. Photochem.* **1979**, *10*, 111.
(28) Bazhin, N. M.; Gritsan, N. P.; Korolev, V. V.; Kamyshan, S. V. *J. Lumin.* **1987**, *37*, 87.
(29) Paddon-Row, M. N. *Acc. Chem. Res.* **1994**, *27*, 18.
(30) Newton, M. *Chem. Rev.* **1991**, *91*, 767.
(31) Georgievskii, Yu.; Burshtein, A. I.; Chernobrod, B. *J. Chem. Phys.* **1996**, *105*, 3108.
(32) Burshtein, A. I.; Kofman, A. G. *Chem. Phys.* **1979**, *40*, 289.
(33) (a) Cao, J.; Minichino, C.; Voth, G. A. *J. Chem. Phys.* **1995**, *103*, 1391. (b) Cao, J.; Voth, G. A. *J. Chem. Phys.* **1997**, *106*, 1769. (c) Cao, J.; Jung, Y. *J. Chem. Phys.* **2000**, *112*, 4716.
(34) Topaller, M.; Makri, N. *J. Chem. Phys.* **1995**, *102*, 460.